A Role for Dystonia-Associated Genes in Spinal GABAergic Interneuron Circuitry

Juliet Zhang[1,2,10], **Jarret A.P. Weinrich**[1,3,9,10], **Jeffrey B. Russ**[1,2,4], **John D. Comer**[1,2,4], **Praveen K. Bommareddy**[1], **Richard J. DiCasoli**[1], **Christopher V.E. Wright**[5], **Yuqing Li**[6], **Peter J. van Roessel**[7], and **Julia A. Kaltschmidt**[1,2,3,8,11,*]

[1]Developmental Biology Program, Sloan Kettering Institute, New York, NY 10065, USA

[2]Neuroscience Program, Weill Cornell Graduate School of Medical Sciences, Weill Cornell Medicine, New York, NY 10065, USA

[3]Biochemistry, Cell and Molecular Biology Program, Weill Cornell Graduate School of Medical Sciences, Weill Cornell Medicine, New York, NY 10065, USA

[4]Weill Cornell/Rockefeller/Sloan Kettering Tri-Institutional MD-PhD Program, New York, NY 10065, USA

[5]Vanderbilt University Program in Developmental Biology, Vanderbilt Center for Stem Cell Biology, Department of Cell and Developmental Biology, Vanderbilt University, Nashville, TN 37232, USA

[6]Department of Neurology, College of Medicine, University of Florida, Gainesville, FL 32610, USA

[7]Department of Psychiatry and Behavioral Sciences, Stanford University School of Medicine, Stanford, CA 94305, USA

[8]Department of Neurosurgery, Stanford University School of Medicine, Stanford, CA 94305, USA

SUMMARY

Spinal interneurons are critical modulators of motor circuit function. In the dorsal spinal cord, a set of interneurons called GABApre presynaptically inhibits proprioceptive sensory afferent terminals, thus negatively regulating sensory-motor signaling. Although deficits in presynaptic

*Correspondence: jukalts@stanford.edu.
[9]Present address: Department of Anatomy, University of California, San Francisco, San Francisco, CA 94158, USA
[10]These authors contributed equally
[11]Lead Contact

inhibition have been inferred in human motor diseases, including dystonia, it remains unclear whether GABApre circuit components are altered in these conditions. Here, we use developmental timing to show that GABApre neurons are a late Ptf1a-expressing subclass and localize to the intermediate spinal cord. Using a microarray screen to identify genes expressed in this intermediate population, we find the kelch-like family member Klhl14, implicated in dystonia through its direct binding with torsion-dystonia-related protein Tor1a. Furthermore, in *Tor1a* mutant mice in which Klhl14 and Tor1a binding is disrupted, formation of GABApre sensory afferent synapses is impaired. Our findings suggest a potential contribution of GABApre neurons to the deficits in presynaptic inhibition observed in dystonia.

In Brief
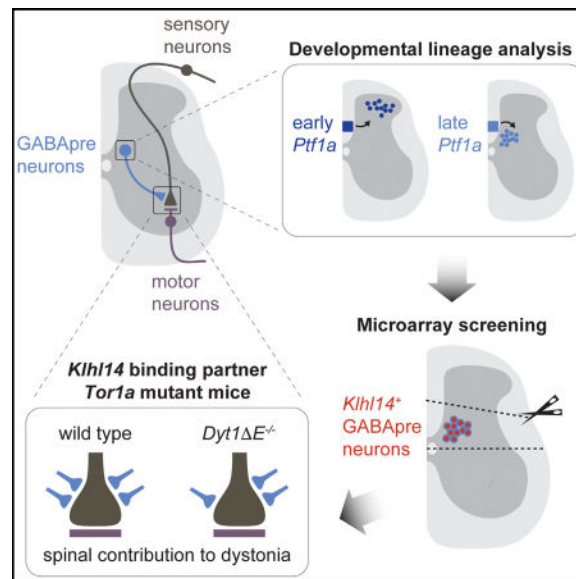
GABApre spinal interneurons gate sensory inputs onto motor neurons. Zhang et al. localize GABApre neurons to the intermediate spinal cord and show that these interneurons express hereditary dystonia-related genes *Klhl14* and *Tor1a*. In *Tor1a* mutant mice, GABApre synapse formation is disrupted, suggesting that spinal circuits may be affected in dystonia.

INTRODUCTION

Spinal interneurons are key components of the neuronal circuits that encode vertebrate motor control. Dysfunction of inhibitory interneurons is thought to contribute to the symptoms of diverse neurologic conditions, including spinal cord injury, amyotrophic lateral sclerosis (ALS), and cerebral palsy (Tillakaratne et al., 2000; Achache et al., 2010; Raynor and Shefner, 1994) and may underlie locomotor defects associated with these conditions such as spasticity and impaired control of voluntary movement (Achache et al., 2010; Comi et al., 2005; Wootz et al., 2013). Yet although injury or disease-related functional deficits have been identified in physiologically defined spinal circuits, little is known about the potential involvement of specific, molecularly defined classes of inhibitory spinal interneurons in the pathophysiology of locomotor disorders.

The monosynaptic stretch reflex, one of the simplest and best-defined spinal circuits, ensures a balance between muscle stretch and contraction, fine-tuning muscle tension to the demands of locomotion. In this circuit, the state of muscle stretch is relayed via proprioceptive sensory neurons to spinal motor neurons, which drive the reflex contraction of the muscle of origin (Eccles et al., 1957; Mears and Frank, 1997). Activity across the sensory-motor synapse is presynaptically modulated by a specific class of GABAergic inhibitory interneurons, called GABApre neurons, that form presynaptic, axo-axonic synapses with sensory afferent terminals (Windhorst, 1996; Rudomin and Schmidt, 1999; Betley et al., 2009; Hughes et al., 2005). GABApre neurons dampen the natural oscillatory movement that would otherwise occur because of the inherent nature of sensory feedback in the spinal reflex circuit, and in their absence, goal-directed movement is severely limited (Fink et al., 2014; Stein and O uztöreli, 1976).

Evidence for the involvement of GABApre interneurons in motor diseases comes from physiologic studies in individuals with dystonia, Huntington's disease, and Parkinson's disease. People affected by such illnesses display deficits in presynaptic inhibition of spinal sensory-motor activity as measured by the Hoffman reflex (H-reflex) (Knikou, 2008), implicating the involvement of GABApre neurons in their disease pathology (Nakashima et al., 1989; Panizza et al., 1990; Roberts et al., 1994; Priori et al., 1995, 2000; Morita et al., 2000). However, we know little about what role the GABApre-sensory microcircuit may play in disease states and whether changes in this circuitry may reflect causes of, or adaptations to, motor illnesses.

Recent work elucidating the developmental origin, connectivity, and synaptic composition of GABApre neurons demonstrates how H-reflex changes in motor disease may be linked to deficits of presynaptic inhibition. GABApre boutons can be identified by specific molecular markers, including the GABA synthetic enzymes GAD65 and GAD67, and the Ca^{2+} sensor synaptotagmin-1 (Syt1) (Betley et al., 2009; Hughes et al., 2005). These markers have been used to show that the targeting of GABApre boutons to sensory afferent terminals is mediated in part by an adhesive signaling complex including contactin-5/CASPR4, expressed in sensory neurons, and NrCAM, expressed in GABApre neurons (Ashrafi et al., 2014). Loss of any of these factors results in a decrease in the number of GABApre-sensory afferent synapses (Ashrafi et al., 2014). The molecular composition of GABApre boutons has further been shown to be closely regulated, and alterations in the molecular composition of GABApre boutons lead to alterations in functional presynaptic inhibition (Mende et al., 2016). Changes in presynaptic inhibition witnessed in different motor diseases may therefore be linked to deficits in the assembly, molecular composition, or maintenance of the GABApre microcircuit.

GABApre interneurons can be distinguished by the expression of pancreas transcription factor (Ptf) 1a (Betley et al., 2009; Hughes et al., 2005). However, although *Ptf1a* marks all dorsal inhibitory interneurons, including GABApre neurons, there is as of yet no specific marker for this functionally distinct GABAergic interneuron subtype. Furthermore, the requirement of Ptf1a for fate specification of dorsal GABAergic interneurons spans the earlyborn dI4 and late-born dIL[A] progenitor populations (Glasgow et al., 2005; Wildner et al., 2006). Although previous work suggests that inhibitory interneurons born during these

two major waves of neurogenesis in the dorsal spinal cord give rise to molecularly and functionally distinct interneuron populations (Gross et al., 2002; Müller et al.,2002;Caspary and Anderson, 2003; Helms and Johnson, 2003; Lai et al., 2016), the developmental domain and settling position of GABApre neurons remains relatively unknown.

In this study, we used a conditional genetic strategy for lineage tracing and the timeline of *Ptf1a* expression to localize the cell bodies of GABApre neurons to the intermediate spinal cord. We further used a comparative microarray analysis to uncover genes specifically enriched by interneurons in the intermediate spinal cord. In an effort to link motor disease pathologies and GABApre circuitry, we focused on genes potentially involved in motor diseases and identified the dystonia-related kelch-like family member protein *Klhl14* as a marker of GABApre interneurons. To explore genetic networks related to *Klhl14* activity in GABApre interneuronal circuitry, we used a mutant mouse (*Dyt1 E*) in which the binding partner of *Klhl14*, the more broadly expressed *Tor1a*, is mutated (Dang et al., 2005).*Tor1a* encodes a protein in the ATPase family that is involved in protein folding and trafficking (Breakefield et al., 2008; Charlesworth et al., 2013). Humans with dystonia related to analogous mutation in the *TOR1A* gene further show deficits in presynaptic inhibition (Edwards et al., 2003). Analysis of *Dyt1 E* mice showed a decrease in GABApre bouton number on sensory afferent terminals, suggesting that the Tor1a/Klhl14 pathway plays a role in GABApre-sensory afferent synapse formation. Taken together, our findings help define the organization and genetic profile of a discrete set of intermediate spinal inhibitory interneurons that exert significant modulatory action during motor behavior. More broadly, our results suggest a link between a pathophysiologically relevant genetic lesion and deficits in the synaptic connectivity of a defined spinal neuronal circuit.

RESULTS

Late *Ptf1a* Expression Distinguishes GABApre Neurons

We first addressed the developmental origins of the GABApre interneuron population. The postmitotic bHLH transcription factor *Ptf1a* is expressed by dorsal inhibitory interneurons from embryonic day (e) 10.5 until e13.5 (Figures S1A–S1H') (Glasgow et al., 2005), which corresponds to both early (dI4) and late (dIL^A) waves of neurogenesis (Gross et al., 2002; Müller et al., 2002). *Ptf1a^{Cre}* mice carrying the tdTomato reporter *ROSA26$^{CAG-lsl-tdTomato}$* (Madisen et al., 2010) have previously been shown to label superficial dorsal and intermediately located cell bodies in the developing spinal cord, as well as GABApre boutons on vGluT1-expressing (vGluT1^{ON}) sensory terminals (Figures 1B, 1C, and 1N) (Betley et al., 2009). tdTomato-expressing (tdTomato^{ON}) GABApre boutons on vGluT1^{ON} sensory terminals express both isoforms of the GABA-synthetic enzymes GAD65 and GAD67, known markers of GABApre neurons (Figures 1D and 1E) (Betley et al., 2009; Hughes et al., 2005).

We sought to determine whether GABApre neurons could be assigned to either early or late temporal domains of *Ptf1a* expression (Figures S1A–S1H'). To accomplish this, we used an inducible *Ptf1a^{CreER}* mouse line (Pan et al., 2013) crossed to *ROSA26$^{CAG-lsl-tdTomato}$* mice and injected tamoxifen (TM) at different time points (Nguyen et al., 2009) (Figure 1A). We found that injecting 100 μg/g TM at e9.5 or e12.5 gives rise to tdToma-to^{ON} *Ptf1a*-derived

neurons. Neurons labeled in response to e9.5 TM do not project ventrally (Figures 1G–1I). In contrast, neurons labeled in response e12.5 TM project ventrally, form contacts on vGluT1[ON] sensory terminals (Figure 1K) and express GAD65 (Figure 1L) and GAD67 (Figure 1M). We thus interpret that TM injections into *Ptf1a*[CreER]*; R26*[tdTomato] mice at e12.5 label GABApre interneurons and that GABApre neurons must therefore express Ptf1a during the late (dIL[A]) wave of inhibitory interneuron neurogenesis.

To clarify the location of GABApre neurons, we assessed if late-expressing *Ptf1a*-derived neurons acquire a different cell body position compared with early-expressing *Ptf1a*-derived neurons. TM injection at e9.5 predominately labels neurons localized to superficial layers of the dorsal horn (Figures 1F and 1O), while TM injection at e12.5 also labels neurons localized to the intermediate spinal cord (Figures 1J and 1P). Taken together, the differences in the spatial distributions of early and late *Ptf1a*-expressing neurons and synapses suggest that two distinct subdomains of interneurons arise from the Ptf1a-expressing domain, the latter of which comprises the GABApre neuron population in the intermediate spinal cord.

Screen for Motor Disease-Associated Markers Enriched in the Intermediate Spinal Cord

On the basis of these and on previous results suggesting that GABApre neurons reside in the intermediate spinal cord (Betley et al., 2009; Jankowska et al., 1981; Hughes et al., 2005), we sought to compare gene expression profiles of the intermediate spinal cord with more dorsal and more ventral regions in an attempt to uncover potential links between novel GABApre enriched genes and previously identified motor disease associated genes. We and others previously showed that *Gad65::*[N45]*GFP* mice label putative GABApre neurons (Betley et al., 2009; Hughes et al., 2005). Thus the lumbar spinal cords of postnatal day (p) 6 *Gad65::*[N45]*GFP* mice were microdissected into dorsal, intermediate, and ventral regions, where GFP fluorescence was used to delineate the boundaries between the different regions (Figure 2A, inset). Gene expression in each region was quantified by microarray, the results of which were processed to allow a comparative analysis of expression levels between intermediate versus ventral and intermediate versus dorsal regions.

We found 268 genes to be at least 2-fold up-or downregulated on comparison of both intermediate versus ventral and intermediate versus dorsal tissue (Figure 2A, Q1, Q2, Q3, and Q4; p   0.05, ANOVA). From this list, 61 genes were greater than 2-fold upregulated in the intermediate spinal cord compared with both the dorsal and ventral spinal cord (Figure 2A, Q1; p   0.05, ANOVA; Table S1). This subset encodes proteins with diverse molecular functions, including DNA binding, ion binding, nucleotide binding, receptors, as well as those with unknown function (Figure 2B). From this list of 61 genes, we evaluated the spinal expression patterns in p4 mice using the Allen Brain Atlas (http://www.brain-map.org). We found 11 candidates to be exclusively expressed in the intermediate spinal cord (Figure 2C, highlighted in Table S1). We assessed these candidates for those that were previously reported to be involved in motor disease. One of these genes was the kelch-like family member protein *Klhl14*. KLHL14 has been implicated in dystonia because of its direct binding of the torsin family 1, member A (TOR1A) (Giles et al., 2009). A dominant single-amino acid mutation in *TOR1A, DYT1 E*, is highly implicated in early-onset generalized

dystonia in humans, leading to sporadic and painful sustained muscle contractions involving both agonist and antagonist muscles (Ozelius et al., 1997; Breakefield et al., 2008).

Klhl14 Is Expressed in *Ptf1a*-Domain-Derived Interneurons of the Intermediate Spinal Cord

Klhl14 has previously been shown to be expressed in the intermediate e18.5 spinal cord (Wildner et al., 2013). We assessed the expression pattern of *Klhl14* during late embryonic and early postnatal stages using in situ hybridization, a time period during which the GABApre-sensory circuit forms (Betley et al., 2009). At late embryonic (e18.5) (Figure 3A) and early postnatal ages (p5 and p10) (Figures 3B and 3C), *Klhl14* was expressed in a restricted domain of the intermediate spinal cord, close to the central canal, throughout the rostro-caudal extent of the lumbar spinal cord (Figure 3D, red arrows). We did not detect *Klhl14* signal in dorsal root ganglia (DRG), suggesting that *Klhl14* is not expressed in sensory neurons (Figure 3D, black arrow).

We next asked if *Klhl14* was expressed in GABAergic inhibitory interneurons. The transcription factor *Ptf1a* is required for GABAergic neurotransmitter fate, and in the absence of *Ptf1a*, the precursors of spinal GABAergic interneurons give rise to excitatory glutamatergic neurons instead (Glasgow et al., 2005). In *Ptf1a* mutant spinal cords (*Ptf1a$^{Cre/Cre}$*) (Kawaguchi et al., 2002), we observed no spinal expression of *Klhl14* (Figure 3E), as previously reported (Wildner et al., 2013). To further test whether *Klhl14* is expressed in *Ptf1a*-derived GABAergic interneurons, we labeled *Ptf1a*-derived neurons by intercrossing the *Ptf1a^{Cre}* driver line with mice carrying a Thy1^{YFP} fluorescent protein reporter line (Buffelli et al., 2003) and performed dual immunohistochemistry/in situ hybridization using an anti-GFP antibody and an antisense *Klhl14* RNA probe. We found that *Klhl14* expression strongly overlapped with YFP-expressing (YFP^{ON}) *Ptf1a*-derived neurons in the intermediate spinal cord (Figure 3F). Given the absence of *Klhl14* expression in *Ptf1a* mutants, we attribute the detection of *Klhl14* in neurons that are YFP^{OFF} to the known mosaicism of the *Ptf1a^{Cre}; Thy1^{YFP}* genotype (Betley et al., 2009). Taken together, these results suggest that *Klhl14* is expressed in Ptf1a-derived interneurons of the intermediate spinal cord.

To determine whether *Klhl4* labels GABApre neurons, we injected TM at e12.5 into *Ptf1a^{CreER}; R26^{tdTomato}* mice and assessed co-expression of *Klhl14* and tdTomato. We found that *Klhl14* expression strongly overlapped with tdTomato^{ON} *Ptf1a*-derived neurons in the intermediate spinal cord (Figures 3G and Figure S2A–S2C). We performed analogous co-expression analysis for tdTomato and *Gad2* transcript, the primary molecular marker for GABApre neurons, and similarly saw strong co-localization in the intermediate spinal cord (Figures 3G). The domains of co-expression of *Klhl14* and tdTomato, as well as *Gad2* and tdTomato, were highly overlapping (Figure 3G), further suggesting that *Klhl14* is expressed in GABApre neurons.

No Loss of Ptf1a-Derived Neurons in the Intermediate Spinal Cord of *Tor1a* Mutants

KLHL14 is a known binding partner of the dystonia 1 protein TOR1A (Giles et al., 2009). Deletion of a single glutamic acid residue in the C-terminal region of TOR1A (ΔE) severely disrupts binding to KLHL14 (Giles et al., 2009), and in humans, this mutation causes early-

onset generalized torsion dystonia in an autosomal dominant manner (Ozelius et al., 1997; Breakefield et al., 2008). We therefore assessed whether the Tor1a/Klhl14 pathway could have a functional role in GABApre circuit formation. Analysis of Tor1a expression revealed that it is expressed broadly, including the majority of *Ptf1a*-derived interneurons in the intermediate spinal cord (Figures 4A and 4B), as well as in proprioceptive sensory neurons in the DRG (Figure 5A). These data confirm that Tor1a and its binding partner Klhl14 are expressed in putative GABApre interneurons in the intermediate spinal cord.

One of the major hallmarks of many motor diseases is targeted death of highly specialized cell types (Gorman, 2008; Liang et al., 2014). Given that Klhl14 and Tor1a localize to putative GABApre neurons, we next assessed whether GABApre neuron cell death results from dysfunction in the Tor1a/Klhl14 pathway. As the homozygous *Dyt1 ΔE* mutation is embryonic lethal, we used heterozygous male mice (Dang et al., 2005), which are viable and display motor abnormalities such as defects in beam walking and hyperactivity at 6 months of age (Dang et al., 2005) as well as marked increase in sustained muscle contractions and co-contraction of functionally opposed muscles suggestive of dystonia (DeAndrade et al., 2016). To label putative GABApre neurons, we generated *Ptf1a^{Cre}; R26^{tdTomato}* mice carrying either the *Dyt1 ΔE* or wildtype (WT) allele and quantified the number of fluorescently labeled neurons in the intermediate spinal cord (Figures 4C and 4D). We saw no difference in the number of tdTomato^{ON}, *Ptf1a*-derived neurons in the intermediate region in *Dyt1 ΔE* compared with control mice (Figure 4E; control: 25.36 ± 3.84 neurons, n = 11 images, three mice; *Dyt1 ΔE*: 24.54 ± 5.17 neurons, n = 13 images, three mice; p = 0.66, two-way ANOVA). We therefore conclude that GABApre neuron number is unchanged in the *Dyt1 ΔE* mutation.

Increased Number of Proprioceptive Terminals in *Dyt1 ΔE* Mice

Because Tor1a is also expressed in proprioceptive neurons of the DRG, we assessed sensory-motor connectivity in *Dyt1 ΔE* mice. We observed no difference in the number of proprioceptive sensory neurons in *Dyt1 ΔE* mice compared with WT (Figures 5A and 5B; control: 142.1 ± 14.1 neurons/DRG, n = 426 neurons, three mice; *Dyt1 ΔE*: 173.4 ± 18.4 neurons/DRG, n = 520 neurons, three mice; p = 0.084, repeated-measures two-way ANOVA). However, the number of vGluT1^{ON} sensory afferent terminals in lamina IX was increased in *Dyt1 ΔE* mice compared with control mice at p21 (Figures 5C and 5E; 1.28-fold; control: 2.81 ± 0.40 terminals/1,000 μm^3, n = 2,300 terminals, three mice; *Dyt1 ΔE*: 3.58 ± 0.75 terminals/ 1,000 μm^3, n = 2,808 terminals, three mice; p < 0.0001, oneway nested ANOVA). Concomitantly, sensory afferent terminal volume was reduced in *Dyt1 ΔE* mice (Figures 5D and 5E; 0.77-fold; control: 3.92 ± 3.70 μm^3, n = 2,300 terminals, three mice; *Dyt1 ΔE*: 3.01 ± 2.82 μm^3, n = 2,808 terminals, three mice; p < 0.0001, one-way nested ANOVA). This reduction was driven largely by an increase in the number of sensory afferent terminals with a volume smaller than 5 μm^3 (Figure 5E). The alignment of the post-synaptic density marker, Shank1a, with vGlut1^{ON} sensory afferent terminals was unchanged, indicating that sensory-motor synapse formation remains normal (Figures 5F–5H) (Betley et al., 2009). We last assessed for potential changes in sensory activity using GABApre terminal expression of GAD67 as a proxy measure. We previously showed that activity deficits in sensory neurons result in decreased GAD67 synaptic accumulation (Mende et al.,

2016). We found no change in GAD67 intensity in GABApre terminals of *Dyt1 E* mice
(Figure 5P; control: 1.00 ± 0.60 normalized GAD67 fluorescence intensity, n = 271
synapses, three mice; *Dyt1 E*: 0.94 ± 0.55 GAD67 fluorescence intensity, n = 212 synapses,
three mice; p = 0.215, nested ANOVA). The unchanged level of GAD67 suggests that
sensory activity is unperturbed in *Dyt1 E* mice.

GABApre Bouton Number Is Decreased in *Tor1a* Mutant Mice

We next assessed whether GABApre synaptic organization was affected in *Dyt1 E* mice.
We used the co-expression of GAD65 and GAD67 (GAD65[ON]/GAD67[ON]) abutting
vGluT1[ON] sensory terminals to label GABApre-sensory afferent synapses (Figure 5F)
(Betley et al., 2009). We quantified the number of GAD65[ON]/GAD67[ON] boutons at p21
when locomotor circuits have finished developing (Figures 5L–5M′), as well as at 6 months
(Figures 5N–5O′) when a behavioral motor defect is first observed in *Dyt1 E* mice (Dang et
al., 2005). We found 20.3% and 27.4% reductions in the number of GAD65[ON]/GAD67[ON]
boutons on vGluT1[ON] sensory terminals in *Dyt1 E* mice compared with WT controls at p21
(Figures 5I, 5K, and 5L–5M′; WT: 2.35 ± 2.12, n = 287 boutons, three mice; *Dyt1 E*: $1.87
\pm 1.67$, n = 287 boutons, three mice; $p < 0.01$, one-way nested ANOVA) and 6 months,
respectively (Figures 5J and 5N–5O′; WT: 2.51 ± 2.22, n = 287 boutons, three mice;
Dyt1 E: 1.82 ± 1.78, n = 287 boutons, three mice; $p < 0.0001$, one-way nested ANOVA).
We did not find any changes in the number of GAD65- or GAD67-only-expressing terminals
apposing vGluT1[ON] sensory afferent terminals (data not shown). These findings suggest that
the Tor1a/Klhl14 pathway is required for organizing the proper number of GABApre
boutons per sensory terminal.

Dyt1 E mice have been shown to have deficits in synaptic vesicle recycling and synaptic
protein stabilization in neural tissues such as the hippocampus and cerebellum (Granata et
al., 2011; Kim et al., 2010). However, we do not see changes in the fluorescence intensity of
synaptic vesicle marker Syt1 in *Dyt1 E* mice compared with controls at p21, as measured
by immunofluorescence confocal imaging (Figure 5Q; relative fluorescence intensity
change: control: 1.00 ± 0.64, n = 369 boutons, three mice; *Dyt1 E*: 1.16 ± 0.74, n = 578
boutons, three mice; p = 0.14, one-way nested ANOVA). This finding, together with the
stability of GABApre terminal GAD67 intensity described above (Figure 5P), suggests that
GABApre synaptic differentiation remains unaltered.

DISCUSSION

Spinal interneurons are essential for modulating locomotor behavior, but their potential
involvement in many motor diseases is unclear. Deficits in presynaptic inhibition of
proprioceptive sensory afferents have been observed in human patients with movement
disorders or focal motor deficits (Nakashima et al., 1989; Panizza et al., 1990; Priori et al.,
2000; Berardelli et al., 1998), suggesting a potential role for spinal GABApre interneurons
in the pathophysiology of such disorders. In this study, we found that late Ptf1a-expressing
neurons give rise to the GABApre interneuron subpopulation. Guided by their localization,
we performed a microarray screen and identified that the kelch-like family member protein
Klhl14 is expressed in GABApre interneurons. Our findings reveal that mutation of the

Klhl14 binding partner Tor1a, a hereditary dystonia-related gene, at a site that disrupts binding to Klhl14, leads to measurable deficits in GABApre-sensory neuron connectivity. Our data thereby suggest a role for dystonia-related genes in the development of spinal sensory-motor circuitry.

Position and Developmental Origin of GABApre Interneurons

In this work, we provide evidence that the cell bodies of ventrally projecting GABApre interneurons are located in the intermediate spinal cord and demonstrate that their segregation to this region correlates with the developmental timing of transcription factor expression. Interneuronal diversification in the spinal cord begins embryonically with discrete progenitor domains giving rise to specific precursor populations. A first wave of neurogenesis (e10–e11.5) gives rise to dorsal inhibitory interneurons of the dI4 domain, and a second wave of neurogenesis (e12–e14.5) generates dorsal inhibitory interneurons of the dIL[A] domain (Gross et al., 2002; Müller et al., 2002). Previous positional studies suggest that the majority of dI4 interneurons remain in the deep dorsal horn, while dIL[A] interneurons migrate to the superficial dorsal horn (Müller et al., 2002; Gross et al., 2002; Helms and Johnson, 2003; Caspary and Anderson, 2003). Our molecular labeling and developmental timing studies now identify GABApre interneurons as localized to the intermediate spinal cord and emerging from dIL[A] during the second wave of neurogenesis. This appears to contradict the prevalent model that the later-born dIL[A] interneurons populate the superficial dorsal horn, but it is consistent with the findings of Nornes and Carry (1978), whose autoradiographic studies show that later-born interneurons (e12–e13) populate both superficial dorsal and medial regions of the dorsal lumbar spinal cord and that only medially located cells are marked by labeling at e14.

Timed Transcription Factor Expression in Neuronal Circuitry

Ptf1a is required for the development of inhibitory neurons throughout the CNS (Jusuf and Harris, 2009; Pascual et al., 2007). Previous molecular-anatomical work inferred at least two different populations of Ptf1a-expressing synapses (Betley et al., 2009): (1) a peptidergic and glycinergic one that forms axo-axonic contacts on cutaneous sensory afferent terminals in the dorsal spinal cord and (2) the GABApre terminals that are neither glycinergic nor peptidergic but express GAD65, GAD67, and Syt1 and form direct axo-axonic connections with proprioceptive sensory afferent terminals in the intermediate and ventral spinal cord (Betley et al., 2009; Hughes et al., 2005). Electrophysiological evidence further suggests that these distinct populations of synapses arise from spatially segregated cell populations with different functions. A dorsal interneuron population is thought to be involved in presynaptic inhibition of cutaneous sensory afferent terminals in the dorsal spinal cord, while an intermediate population participates in presynaptic inhibition of proprioceptive sensory afferent terminals in the intermediate and ventral spinal cord (Jankowska et al., 1981). An intermediate location of GABApre neurons is also suggested by co-expression of the GABApre hallmark genes *Gad65* and *Gad67* in neuronal cell bodies of the intermediate spinal cord (Betley et al., 2009), and labeling of GAD65-GFP-expressing cell bodies in the intermediate spinal cord following injection of a tracer dye into the ventral motor column to which GABApre neurons project (Hughes et al., 2005). We now identify GABApre

interneurons as an intermediate population distinct from other Ptf1a-expressing dorsal GABAergic interneurons.

Our results suggest a relationship between the timing of transcription factor expression and neuronal settling position, circuit connectivity, and function. As such, our work supports and extends previous findings showing that multiple aspects of neuronal fate, including migratory behavior and ultimate cell body positioning, are associated with timing of neurogenesis (Tripodi et al., 2011; Benito-Gonzalez and Alvarez, 2012; Stam et al., 2012; Tripodi and Arber, 2012). Several recent findings further suggest that cell body position correlates with sensory input connectivity of both motor neurons (Sürmeli et al., 2011) and interneurons (Tripodi et al., 2011; Bikoff et al., 2016). The dorsal-medial location of GABApre cell bodies positions them in a region of spinal cord densely innervated by descending corticospinal tract axons (Bareyre et al., 2005; Russ et al., 2013) and supports a role for GABApre interneurons in integrating descending cortical inputs into the regulation of the sensory-motor reflex circuit (Azim et al., 2014). The late expression of Ptf1a could thereby play a dual role in (1) guiding GABApre neurons to a settling position within the spinal cord that ensures proper input from supraspinal, spinal, and sensory neurons and (2) initiating signaling cascades that determine their efferent proprioceptive targeting.

Tor1a Function in GABApre Circuitry

Our study further supports a role for Tor1a in GABAergic synaptogenesis, given the decrease in GABApre-sensory afferent synapses we observe in *Dyt1 ΔE* mice. Tor1a is a broadly expressed AAA+-class ATPase, intracellularly localized to the nuclear envelope and endoplasmic reticulum, postulated to function as a chaperone protein and in the modification and processing of protein complexes through secretory pathways. Tor1a is enriched in developing neuronal tissues and has been identified in the cytosol and neurites of neurons, including both the axonal and dendritic compartments of GABAergic Purkinje cells in the cerebellum (Puglisi et al., 2013; Breakefield et al., 2008). Functionally, Tor1a has been shown to play a role in synaptic vesicle recycling (Granata et al., 2008, 2011) and in synaptic vesicle release (Yokoi et al., 2013). Structurally, in mouse cerebellum, there is a decrease in inhibitory synaptic contacts on Purkinje cells in both *Tor1a*^{+/−} mice and mice carrying the human *Dyt1 ΔE* mutation, suggesting that GABAergic synaptogenesis is compromised in the presence of mutant Tor1a (Vanni et al., 2015).

How dysfunction of Tor1a contributes to the decreased number of GABApre-sensory afferent synapses remains an outstanding question. The *DYT ΔE* mutation disrupts binding of TOR1A to KLHL14 (Giles et al., 2009). Little is known about Klhl14, yet another member of the Kelch-like protein family, Klhl1, modulates voltage-gated calcium channels (Nemes et al., 2000) and regulates neurite and cellular process extension (Seng et al., 2006; Jiang et al., 2007). Knockdown of Klhl1 in rat hippocampal cultures results in decreased numbers of excitatory and inhibitory synapses (Perissinotti et al., 2015). The loss of synapses seen in *Dyt1 ΔE* mice hints that Klhl14 may have a similar role to Klhl1. If Klhl14 binds actin like Klhl1 (Nemes et al., 2000), this would support models of Tor1a's function at the interface of synaptic membrane recycling and local cytoskeletal dynamics (Granata et al., 2009). Given that the *Dyt1 ΔE* phenotype of decreased GABApre-sensory afferent synapse number is

strikingly similar to that seen following deletion of Ig-superfamily adhesion molecules expressed in GABApre interneurons or their sensory afferent partners (Ashrafi et al., 2014), it is further tempting to speculate that adhesive signaling may be affected by *Dyt1 E*. Tor1a has been shown to interact with components of the dystrophin-associated glycoprotein complex (DGC) (Esapa et al., 2007). Dystroglycan, a component of the DGC, binds to neurexin (Sumita et al., 2007) and indirectly interacts with NL2 (Sugita et al., 2001), an adhesion molecule also found to localize to sensory neurons (Ashrafi et al., 2014). This suggests a potential role for Tor1a in adhesion molecule localization in the GABApre-sensory neuron connectivity (Puglisi et al., 2013; Patrizi et al., 2008).

Our data cannot formally distinguish whether Tor1a functions in GABApre interneurons or in sensory neurons to influence GABApre-sensory afferent synapse number. Tor1a is expressed in both GABApre interneurons and proprioceptive sensory neurons, while its reported binding partner Klhl14 is not expressed in sensory neurons. This may point to different functions for Tor1a in these distinct neuronal populations. The fact that the *Dyt1 E* mutation abolishes binding of Klhl14 to Tor1a suggests that the GABApre phenotype we observe reflects Klhl14's function in GABApre interneurons. Tor1a likely functions in oligomers, however, and its ability to bind itself may also be compromised by the *Dyt1 E* mutation (Pham et al., 2006). We do see an increase in the number of smaller volume sensory afferent terminals in *Dyt1 E* mice, leading to the possibility that the decrease in the number of GABApre boutons per sensory afferent terminal is due to an increased number of smaller sensory afferent terminals, which are known to have fewer GABApre boutons (Pierce and Mendell, 1993; Betley et al., 2009). However, estimating the loss of GABApre boutons due to the size principle using previously published data (Pierce and Mendell, 1993) would account for an approximately 7% decrease in GABApre synapses per sensory afferent terminal and therefore would not explain the markedly greater GABApre bouton loss seen in *Dyt1 E* mice (see Supplemental Experimental Procedures). This analysis, together with our finding that intensity of GABApre terminal GAD67 is unchanged—suggesting against alterations in sensory afferent activity state— leads us to see as unlikely the possibility that GABApre terminal number is decreased due to a non-autonomous effect of Tor1a in sensory neurons.

Tor1a is known to be expressed throughout the CNS, including the cerebral cortex, basal ganglia, midbrain, and cerebellum (Granata et al., 2009). As such, a further possibility is that Tor1a mutation generates a non-cell-autonomous synaptic phenotype via function outside the GABApre-sensory microcircuit, for example in CNS regions that send descending projections into the spinal cord. GABApre interneurons receive direct synaptic input from corticospinal tract (CST) axons (Russ et al., 2013), and disruption of CST-GABApre connectivity via cortical lesion results in no change in the number of GABApre-sensory afferent synapses. This is notably in contrast to the *Dyt1 E* mutant phenotype we describe here, in which synaptic number is altered. This contrast leads us to interpret that the Tor1a phenotype does not arise from disruption of descending CST tracts.

The pathophysiology of early-onset primary dystonia has focused on the basal ganglia, particularly the role of cholinergic interneurons in the striatum (Perlmutter and Mink, 2004; Goodchild et al., 2013; Pappas et al., 2015). However, dystonias, including the *DYT1-*

associated early-onset dystonias, are known to be associated with deficits in spinal reciprocal inhibition of the H-reflex, particularly the late phase of this inhibition, believed to be mediated by presynaptic inhibition of sensory afferents (Berardelli et al., 1998; Nakashima et al., 1989; Panizza et al., 1990; Priori et al., 2000). These deficits in presynaptic inhibition have been proposed to reflect alterations in descending corticospinal control of spinal interneurons (Nakashima et al., 1989). Our work, however, identifies the subpopulation of spinal interneurons responsible for presynaptic inhibition and shows that in the presence of dysfunctional Tor1a protein, these interneurons make fewer presynaptic inhibitory contacts on primary sensory afferent neurons. Although the decrement in GABApre terminal number is limited, we know from our previous work that a comparably modest decrease in GABApre terminal GAD67 expression can have a robust impact on measured presynaptic inhibition (Mende et al., 2016). As such, we suggest that deficits in spinal circuits may work in concert with concurrent well-known changes in the basal ganglia, cerebellum, and other supraspinal regions of the CNS to drive motor coordination deficits in dystonia. We propose that focus on the specific interneuron subclasses that constitute the spinal circuitry of movement may better enhance our understanding of the causal factors underlying the complex functional manifestations of motor disease.

EXPERIMENTAL PROCEDURES

Mouse Strains

The following mouse strains were used in this study: $Dyt1^{\Delta E}$ (Dang et al., 2005), $Gad65::^{N45}GFP$ (López-Bendito et al., 2004), $Ptf1a^{Cre}$ (Kawaguchi et al., 2002), $Ptf1a^{CreER}$ (Pan et al., 2013), $R26^{CAG–lox–STOP–tdTomato/+}$ (Jackson Labs, Ai14) (Madisen et al., 2010), and $Thy1^{lox-STOP-YFP}$ (line 15) (Buffelli et al., 2003). $Dyt1^{\Delta E}$ mice were analyzed as heterozygotes, as homozygous animals die (Dang et al., 2005). Experiments conform to the regulatory standards of the Institutional Animal Care and Use Committee of Memorial Sloan Kettering Cancer Center.

TM Injections

TM (T-5648; Sigma-Aldrich) was dissolved in corn oil (C-8267; Sigma-Aldrich) at a final concentration of 20 mg/mL. TM was intraperitoneally injected once into pregnant dams at 9.5 or 12.5 days post-coitus, and pups were harvested at e18.5 or p21. For embryo harvest, 80–100 mg/kg TM was administered at both time points. For postnatal harvest, 20 mg/kg TM was administered at e9.5, and 100 mg/kg TM was administered at e12.5.

Histochemistry

Immunohistochemistry and in situ hybridization on 12-or 20-μm-thick cryostat sections were performed as previously described (Arber et al., 1999; Betley et al., 2009) with the following modification: mice were perfused by peristaltic pump (World Precision Instruments) with a 2% heparin (Butler-Schein) normal saline solution flush, followed by room temperature 4% paraformaldehyde (PFA).

Antibodies were used in 0.3% Triton-X in PBS with 1% BSA or 0.1% PBT with 1% BSA. The following antibodies were used in this study: rabbit anti-GAD65 (1:8,000) (Betley et al.,

2009), mouse anti-GAD67 (1:10,000; Millipore), rabbit anti-GFP (1:1,000; Invitrogen), guinea pig anti-Lmx1b (1:8,000; generously provided by S. Morton and T. Jessell) (Kania et al., 2000), chicken anti-parvalbumin (1:1,000; generously provided by S. Morton and T. Jessell) (de Nooij et al., 2013), rabbit anti-Ptf1a (1:5,000; generously provided by C. Wright), guinea pig anti-RFP (1:2,000; generously provided by N. Betley) (Betley et al., 2013), rabbit anti-RFP (1:1,000; Rockland), rabbit anti-Runx3 (1:4,000; generously provided by S. Morton and T. Jessell) (Chen et al., 2006), rabbit anti-Shank1a (1:1,000; Millipore), rabbit anti-Tor1a (1:600; Millipore), guinea pig anti-vGluT1 (1:32,000) (Betley et al., 2009), and fluorophore-conjugated secondary antibodies (Jackson Labs and Molecular Probes).

In situ hybridization combined with antibody staining was performed as described (Ashrafi et al., 2014). tdTomato or GFP detection in combination with in situ hybridization was performed with additional tyramide signal amplification (TSA) (Perkin-Elmer) of the RFP or GFP antibodies with donkey anti-rabbit HRP-conjugated secondary (1:1,000; Millipore). In situ hybridization of *Gad2* (Russ et al., 2015) and *Klhl14* (generously provided by H. Wildner and C. Birchmeier) (Wildner et al., 2013) was performed with DIG-labeled riboprobes.

Synaptic Quantification

GABApre/vGluT1 synaptic number counts were performed using Leica LASAF software plug-in (version 2.6.0.7266) on z stacks (0.3 μm optical sections) obtained on a Leica TCS SP5 confocal. At least three mice per genotype were analyzed and 99 vGluT1^{ON} sensory afferent terminals were counted per animal. Sensory afferent terminal number, volume, and GABApre fluorescence intensity were analyzed in the 3D image analysis program Imaris. Statistics on Imaris data were performed in MATLAB. Differences between WT/control and mutant mice were determined one-way nested ANOVA unless otherwise indicated, with $p > 0.05$ not significant, $**p < 0.01$, and $****p < 0.0001$. We used box-and-whisker plots where individual data points are either images or synapses within images and scatterplots where data points are individual animals. Data are reported as mean $\pm$ SD.

Candidate Screen

Spinal cords were removed from three p6 *Gad65::^{N45}GFP* mice, embedded in UltraPure L.M.P. agarose (Invitrogen), and vibratome-sectioned at 300 μm. The dorsal, intermediate, and ventral regions were then dissected from each section and flash-frozen on dry ice. RNA was obtained by Trizol extraction and run on an Affymetrix Mouse Genome 430 2.0 Array. Gene expression data were analyzed using the BioConductor suite of tools (http://www.bioconductor.org) in R statistical language (http://www.r-project.org). The data were normalized using standard gcrma function. For each group comparison, differentially expressed genes were sought using limma package with a p value cutoff of 0.05 (adjusted for multiple hypothesis testing) and fold changes of 2. Pathway analysis was done using the functional annotation tool DAVID (https://david.ncifcrf.gov).

Positional Analysis

Probability densities of tdTomato-positive (tdTomato^{ON}) cell body position were calculated in e18.5 *Ptf1a^{Cre}; R26^{tdTomato}* embryos following TM injection at e9.5 and e12.5. Positional coordinates of tdTomato^{ON} cell bodies were obtained using software developed in the laboratory (Russ et al., 2013). The positional coordinates were then processed in R statistical language using the kde2d function from the MASS package. Further computation and graphical display were performed in R using the hexabin package (https://cran.r-project.org/web/packages/hexbin/index.html).

Proprioceptive Sensory Neuron Quantification

Confocal images of DRG sections were evaluated by eye by two separate counters, with the counter blind to genotype. Cells expressing both parvalbumin and Runx3 were counted as proprioceptors. Statistics were generated using repeated-measures two-way ANOVA to compare any effects due to genotype and counter using Prism statistical software.

Supplementary Material

Refer to Web version on PubMed Central for supplementary material.

Acknowledgments

References

Achache V, Roche N, Lamy JC, Boakye M, Lackmy A, Gastal A, Quen-tin V, Katz R. Transmission within several spinal pathways in adults with cerebral palsy. Brain. 2010; 133:1470–1483. [PubMed: 20403961]

Arber S, Han B, Mendelsohn M, Smith M, Jessell TM, Sockana-than S. Requirement for the homeobox gene Hb9 in the consolidation of motor neuron identity. Neuron. 1999; 23:659–674. [PubMed: 10482234]

Ashrafi S, Betley JN, Comer JD, Brenner-Morton S, Bar V, Shimoda Y, Watanabe K, Peles E, Jessell TM, Kaltschmidt JA. Neuronal Ig/Caspr recognition promotes the formation of axoaxonic synapses in mouse spinal cord. Neuron. 2014; 81:120–129. [PubMed: 24411736]

Azim E, Fink AJ, Jessell TM. Internal and external feedback circuits for skilled forelimb movement. Cold Spring Harb. Symp. Quant. Biol. 2014; 79:81–92. [PubMed: 25699987]

Bareyre FM, Kerschensteiner M, Misgeld T, Sanes JR. Trans-genic labeling of the corticospinal tract for monitoring axonal responses to spinal cord injury. Nat. Med. 2005; 11:1355–1360. [PubMed: 16286922]

Benito-Gonzalez A, Alvarez FJ. Renshaw cells and Ia inhibitory interneurons are generated at different times from p1 progenitors and differentiate shortly after exiting the cell cycle. J. Neurosci. 2012; 32:1156–1170. [PubMed: 22279202]

Berardelli A, Rothwell JC, Hallett M, Thompson PD, Manfredi M, Marsden CD. The pathophysiology of primary dystonia. Brain. 1998; 121:1195–1212. [PubMed: 9679773]

Betley JN, Wright CV, Kawaguchi Y, Erdélyi F, Szabó G, Jessell TM, Kaltschmidt JA. Stringent specificity in the construction of a GABAergic presynaptic inhibitory circuit. Cell. 2009; 139:161–174. [PubMed: 19804761]

Betley JN, Cao ZF, Ritola KD, Sternson SM. Parallel, redundant circuit organization for homeostatic control of feeding behavior. Cell. 2013; 155:1337–1350. [PubMed: 24315102]

Bikoff JB, Gabitto MI, Rivard AF, Drobac E, Machado TA, Miri A, Brenner-Morton S, Famojure E, Diaz C, Alvarez FJ, et al. Spinal inhibitory interneuron diversity delineates variant motor microcircuits. Cell. 2016; 165:207–219. [PubMed: 26949184]

Breakefield XO, Blood AJ, Li Y, Hallett M, Hanson PI, Standaert DG. The pathophysiological basis of dystonias. Nat. Rev. Neurosci. 2008; 9:222–234. [PubMed: 18285800]

Buffelli M, Burgess RW, Feng G, Lobe CG, Lichtman JW, Sanes JR. Genetic evidence that relative synaptic efficacy biases the outcome of synaptic competition. Nature. 2003; 424:430–434. [PubMed: 12879071]

Caspary T, Anderson KV. Patterning cell types in the dorsal spinal cord: what the mouse mutants say. Nat. Rev. Neurosci. 2003; 4:289–297. [PubMed: 12671645]

Charlesworth G, Bhatia KP, Wood NW. The genetics of dystonia: new twists in an old tale. Brain. 2013; 136:2017–2037. [PubMed: 23775978]

Chen AI, de Nooij JC, Jessell TM. Graded activity of transcription factor Runx3 specifies the laminar termination pattern of sensory axons in the developing spinal cord. Neuron. 2006; 49:395–408. [PubMed: 16446143]

Comi AM, Johnston MV, Wilson MA. Strain variability, injury distribution, and seizure onset in a mouse model of stroke in the immature brain. Dev. Neurosci. 2005; 27:127–133. [PubMed: 16046846]

Dang MT, Yokoi F, McNaught KS, Jengelley TA, Jackson T, Li J, Li Y. Generation and characterization of Dyt1 DeltaGAG knock-in mouse as a model for early-onset dystonia. Exp. Neurol. 2005; 196:452–463. [PubMed: 16242683]

de Nooij JC, Doobar S, Jessell TM. Etv1 inactivation reveals proprioceptor subclasses that reflect the level of NT3 expression in muscle targets. Neuron. 2013; 77:1055–1068. [PubMed: 23522042]

DeAndrade MP, Trongnetrpunya A, Yokoi F, Cheetham CC, Peng N, Wyss JM, Ding M, Li Y. Electromyographic evidence in support of a knock-in mouse model of DYT1 Dystonia. Mov. Disord. 2016; 31:1633–1639. [PubMed: 27241685]

Eccles JC, Eccles RM, Lundberg A. The convergence of monosynaptic excitatory afferents on to many different species of alpha motoneurones. J. Physiol. 1957; 137:22–50.

Edwards MJ, Huang YZ, Wood NW, Rothwell JC, Bhatia KP. Different patterns of electrophysiological deficits in manifesting and non-manifesting carriers of the DYT1 gene mutation. Brain. 2003; 126:2074–2080. [PubMed: 12821514]

Esapa CT, Waite A, Locke M, Benson MA, Kraus M, McIlhinney RA, Sillitoe RV, Beesley PW, Blake DJ. SGCE missense mutations that cause myoclonus-dystonia syndrome impair epsilon-sarcoglycan trafficking to the plasma membrane: modulation by ubiquitination and torsinA. Hum. Mol. Genet. 2007; 16:327–342. [PubMed: 17200151]

Fink AJ, Croce KR, Huang ZJ, Abbott LF, Jessell TM, Azim E. Presynaptic inhibition of spinal sensory feedback ensures smooth movement. Nature. 2014; 509:43–48. [PubMed: 24784215]

Giles LM, Li L, Chin LS. Printor, a novel torsinA-interacting protein implicated in dystonia pathogenesis. J. Biol. Chem. 2009; 284:21765–21775. [PubMed: 19535332]

Glasgow SM, Henke RM, Macdonald RJ, Wright CV, Johnson JE. Ptf1a determines GABAergic over glutamatergic neuronal cell fate in the spinal cord dorsal horn. Development. 2005; 132:5461–5469. [PubMed: 16291784]

Goodchild RE, Grundmann K, Pisani A. New genetic insights highlight 'old' ideas on motor dysfunction in dystonia. Trends Neurosci. 2013; 36:717–725. [PubMed: 24144882]

Gorman AM. Neuronal cell death in neurodegenerative diseases: recurring themes around protein handling. J. Cell. Mol. Med. 2008; 12(6A):2263–2280. [PubMed: 18624755]

Granata A, Watson R, Collinson LM, Schiavo G, Warner TT. The dystonia-associated protein torsinA modulates synaptic vesicle recycling. J. Biol. Chem. 2008; 283:7568–7579. [PubMed: 18167355]

Granata A, Schiavo G, Warner TT. TorsinA and dystonia: from nuclear envelope to synapse. J. Neurochem. 2009; 109:1596–1609. [PubMed: 19457118]

Granata A, Koo SJ, Haucke V, Schiavo G, Warner TT. CSN complex controls the stability of selected synaptic proteins via a torsin A-dependent process. EMBO J. 2011; 30:181–193. [PubMed: 21102408]

Gross MK, Dottori M, Goulding M. Lbx1 specifies somatosensory association interneurons in the dorsal spinal cord. Neuron. 2002; 34:535–549. [PubMed: 12062038]

Helms AW, Johnson JE. Specification of dorsal spinal cord interneurons. Curr. Opin. Neurobiol. 2003; 13:42–49. [PubMed: 12593981]

Hughes DI, Mackie M, Nagy GG, Riddell JS, Maxwell DJ, Szabó G, Erdélyi F, Veress G, Szucs P, Antal M, Todd AJ. P boutons in lamina IX of the rodent spinal cord express high levels of glutamic acid decar-boxylase-65 and originate from cells in deep medial dorsal horn. Proc. Natl. Acad. Sci. U S A. 2005; 102:9038–9043. [PubMed: 15947074]

Jankowska E, McCrea D, Rudomín P, Sykova E. Observations on neuronal pathways subserving primary afferent depolarization. J. Neurophysiol. 1981; 46:506–516. [PubMed: 7299431]

Jiang S, Seng S, Avraham HK, Fu Y, Avraham S. Process elongation of oligodendrocytes is promoted by the Kelch-related protein MRP2/KLHL1. J. Biol. Chem. 2007; 282:12319–12329. [PubMed: 17324934]

Jusuf PR, Harris WA. Ptf1a is expressed transiently in all types of amacrine cells in the embryonic zebrafish retina. Neural Dev. 2009; 4:34. [PubMed: 19732413]

Kania A, Johnson RL, Jessell TM. Coordinate roles for LIM ho-meobox genes in directing the dorsoventral trajectory of motor axons in the vertebrate limb. Cell. 2000; 102:161–173. [PubMed: 10943837]

Kawaguchi Y, Cooper B, Gannon M, Ray M, MacDonald RJ, Wright CV. The role of the transcriptional regulator Ptf1a in converting intestinal to pancreatic progenitors. Nat. Genet. 2002; 32:128–134. [PubMed: 12185368]

Kim CE, Perez A, Perkins G, Ellisman MH, Dauer WT. A molecular mechanism underlying the neural-specific defect in torsinA mutant mice. Proc. Natl. Acad. Sci. USA. 2010; 107:9861–9866. [PubMed: 20457914]

Knikou M. The H-reflex as a probe: pathways and pitfalls. J. Neurosci. Methods. 2008; 171:1–12. [PubMed: 18394711]

Lai HC, Seal RP, Johnson JE. Making sense out of spinal cord somatosensory development. Development. 2016; 143:3434–3448. [PubMed: 27702783]

Liang CC, Tanabe LM, Jou S, Chi F, Dauer WT. TorsinA hypofunction causes abnormal twisting movements and sensorimotor circuit neurodegeneration. J. Clin. Invest. 2014; 124:3080–3092. [PubMed: 24937429]

López-Bendito G, Sturgess K, Erdélyi F, Szabó G, Molnár Z, Paulsen O. Preferential origin and layer destination of GAD65-GFP cortical interneurons. Cereb. Cortex. 2004; 14:1122–1133. [PubMed: 15115742]

Madisen L, Zwingman TA, Sunkin SM, Oh SW, Zariwala HA, Gu H, Ng LL, Palmiter RD, Hawrylycz MJ, Jones AR, et al. A robust and high-throughput Cre reporting and characterization system for the whole mouse brain. Nat. Neurosci. 2010; 13:133–140. [PubMed: 20023653]

Mears SC, Frank E. Formation of specific monosynaptic connections between muscle spindle afferents and motoneurons in the mouse. J. Neurosci. 1997; 17:3128–3135. [PubMed: 9096147]

Mende M, Fletcher EV, Belluardo JL, Pierce JP, Bommareddy PK, Weinrich JA, Kabir ZD, Schierberl KC, Pagiazitis JG, Mendelsohn AI, et al. Sensory-derived glutamate regulates presynaptic inhibitory terminals in mouse spinal cord. Neuron. 2016; 90:1189–1202. [PubMed: 27263971]

Morita H, Shindo M, Ikeda S, Yanagisawa N. Decrease in presynaptic inhibition on heteronymous monosynaptic Ia terminals in patients with Parkinson's disease. Mov. Disord. 2000; 15:830–834. [PubMed: 11009187]

Müller T, Brohmann H, Pierani A, Heppenstall PA, Lewin GR, Jessell TM, Birchmeier C. The homeodomain factor lbx1 distinguishes two major programs of neuronal differentiation in the dorsal spinal cord. Neuron. 2002; 34:551–562. [PubMed: 12062039]

Nakashima K, Rothwell JC, Day BL, Thompson PD, Shannon K, Marsden CD. Reciprocal inhibition between forearm muscles in patients with writer's cramp and other occupational cramps, symptomatic hemidystonia and hemiparesis due to stroke. Brain. 1989; 112:681–697. [PubMed: 2731027]

Nemes JP, Benzow KA, Moseley ML, Ranum LP, Koob MD. The SCA8 transcript is an antisense RNA to a brain-specific transcript encoding a novel actin-binding protein (KLHL1). Hum. Mol. Genet. 2000; 9:1543–1551. [PubMed: 10888605]

Nguyen MT, Zhu J, Nakamura E, Bao X, Mackem S. Tamox-ifen-dependent, inducible Hoxb6CreERT recombinase function in lateral plate and limb mesoderm, CNS isthmic organizer, posterior trunk neural crest, hindgut, and tailbud. Dev. Dyn. 2009; 238:467–474. [PubMed: 19161221]

Nornes HO, Carry M. Neurogenesis in spinal cord of mouse: an autoradiographic analysis. Brain Res. 1978; 159:1–6. [PubMed: 728790]

Ozelius LJ, Hewett JW, Page CE, Bressman SB, Kramer PL, Shalish C, de Leon D, Brin MF, Raymond D, Corey DP, et al. The early-onset torsion dystonia gene (DYT1) encodes an ATP-binding protein. Nat. Genet. 1997; 17:40–48. [PubMed: 9288096]

Pan FC, Bankaitis ED, Boyer D, Xu X, Van de Casteele M, Magnuson MA, Heimberg H, Wright CV. Spatiotemporal patterns of multipotentiality in Ptf1a-expressing cells during pancreas organogenesis and injury-induced facultative restoration. Development. 2013; 140:751–764. [PubMed: 23325761]

Panizza M, Lelli S, Nilsson J, Hallett M. H-reflex recovery curve and reciprocal inhibition of H-reflex in different kinds of dystonia. Neurology. 1990; 40:824–828. [PubMed: 2330111]

Pappas SS, Darr K, Holley SM, Cepeda C, Mabrouk OS, Wong JM, LeWitt TM, Paudel R, Houlden H, Kennedy RT, et al. Forebrain deletion of the dystonia protein torsinA causes dystonic-like movements and loss of striatal cholinergic neurons. eLife. 2015; 4:e08352. [PubMed: 26052670]

Pascual M, Abasolo I, Mingorance-Le Meur A, Martínez A, Del Rio JA, Wright CV, Real FX, Soriano E. Cerebellar GABAergic progenitors adopt an external granule cell-like phenotype in the absence of Ptf1a transcription factor expression. Proc. Natl. Acad. Sci. USA. 2007; 104:5193–5198. [PubMed: 17360405]

Patrizi A, Scelfo B, Viltono L, Briatore F, Fukaya M, Watanabe M, Strata P, Varoqueaux F, Brose N, Fritschy JM, Sassoe-Pognetto M. Synapse formation and clustering of neuroligin-2 in the absence of GABAA receptors. Proc. Natl. Acad. Sci. USA. 2008; 105:13151–13156. [PubMed: 18723687]

Perissinotti PP, Ethington EA, Almazan E, Martínez-Hernandez E, Kalil J, Koob MD, Piedras-Rentería ES. Calcium current homeostasis and synaptic deficits in hippocampal neurons from Kelch-like 1 knockout mice. Front. Cell. Neurosci. 2015; 8:444. [PubMed: 25610372]

Perlmutter JS, Mink JW. Dysfunction of dopaminergic pathways in dystonia. Adv. Neurol. 2004; 94:163–170. [PubMed: 14509670]

Pham P, Frei KP, Woo W, Truong DD. Molecular defects of the dystonia-causing torsinA mutation. Neuroreport. 2006; 17:1725–1728. [PubMed: 17047461]

Pierce JP, Mendell LM. Quantitative ultrastructure of Ia boutons in the ventral horn: scaling and positional relationships. J. Neurosci. 1993; 13:4748–4763. [PubMed: 7693892]

Priori A, Berardelli A, Mercuri B, Manfredi M. Physiological effects produced by botulinum toxin treatment of upper limb dystonia. Changes in reciprocal inhibition between forearm muscles. Brain. 1995; 118:801–807. [PubMed: 7600096]

Priori A, Polidori L, Rona S, Manfredi M, Berardelli A. Spinal and cortical inhibition in Huntington's chorea. Mov. Disord. 2000; 15:938–946. [PubMed: 11009202]

Puglisi F, Vanni V, Ponterio G, Tassone A, Sciamanna G, Bonsi P, Pi-sani A, Mandolesi G. Torsin A localization in the mouse cerebellar synaptic circuitry. PLoS ONE. 2013; 8:e68063. [PubMed: 23840813]

Raynor EM, Shefner JM. Recurrent inhibition is decreased in patients with amyotrophic lateral sclerosis. Neurology. 1994; 44:2148–2153. [PubMed: 7969975]

Roberts RC, Part NJ, Farquhar R, Butchart P. Presynaptic nhibition of soleus Ia afferent terminals in Parkinson's disease. J. Neurol. Neurosurg. Psychiatry. 1994; 57:1488–1491. [PubMed: 7798978]

Rudomin P, Schmidt RF. Presynaptic inhibition in the vertebrate spinal cord revisited. Exp. Brain Res. 1999; 129:1–37. [PubMed: 10550500]

Russ JB, Verina T, Comer JD, Comi AM, Kaltschmidt JA. Corticospinal tract insult alters GABAergic circuitry in the mammalian spinal cord. Front. Neural Circuits. 2013; 7:150. [PubMed: 24093008]

Russ JB, Borromeo MD, Kollipara RK, Bommareddy PK, Johnson JE, Kaltschmidt JA. Misexpression of ptf1a in cortical pyramidal cells in vivo promotes an inhibitory peptidergic identity. J. Neurosci. 2015; 35:6028–6037. [PubMed: 25878276]

Seng S, Avraham HK, Jiang S, Venkatesh S, Avraham S. KLHL1/MRP2 mediates neurite outgrowth in a glycogen synthase kinase 3beta-dependent manner. Mol. Cell. Biol. 2006; 26:8371–8384. [PubMed: 16982692]

Stam FJ, Hendricks TJ, Zhang J, Geiman EJ, Francius C, Labosky PA, Clotman F, Goulding M. Renshaw cell interneuron specialization is controlled by a temporally restricted transcription factor program. Development. 2012; 139:179–190. [PubMed: 22115757]

Stein RB, Oğuztöreli MN. Tremor and other oscillations in neuromuscular systems. Biol. Cybern. 1976; 22:147–157. [PubMed: 1276248]

Sugita S, Saito F, Tang J, Satz J, Campbell K, Sudhof TC. A stoichiometric complex of neurexins and dystroglycan in brain. J. Cell Biol. 2001; 154:435–445. [PubMed: 11470830]

Sumita K, Sato Y, Iida J, Kawata A, Hamano M, Hirabayashi S, Ohno K, Peles E, Hata Y. Synaptic scaffolding molecule (S-SCAM) membrane-associated guanylate kinase with inverted organization (MAGI)-2 is associated with cell adhesion molecules at inhibitory synapses in rat hippocampal neurons. J. Neurochem. 2007; 100:154–166. [PubMed: 17059560]

Sürmeli G, Akay T, Ippolito GC, Tucker PW, Jessell TM. Patterns of spinal sensory-motor connectivity prescribed by a dorsoventral positional template. Cell. 2011; 147:653–665. [PubMed: 22036571]

Tillakaratne NJ, Mouria M, Ziv NB, Roy RR, Edgerton VR, Tobin AJ. Increased expression of glutamate decarboxylase (GAD(67)) in feline lumbar spinal cord after complete thoracic spinal cord transection. J. Neurosci. Res. 2000; 60:219–230. [PubMed: 10740227]

Tripodi M, Arber S. Regulation of motor circuit assembly by spatial and temporal mechanisms. Curr. Opin. Neurobiol. 2012; 22:615–623. [PubMed: 22417941]

Tripodi M, Stepien AE, Arber S. Motor antagonism exposed by spatial segregation and timing of neurogenesis. Nature. 2011; 479:61–66. [PubMed: 22012263]

Vanni V, Puglisi F, Bonsi P, Ponterio G, Maltese M, Pisani A, Man-dolesi G. Cerebellar synaptogenesis is compromised in mouse models of DYT1 dystonia. Exp. Neurol. 2015; 271:457–467. [PubMed: 26183317]

Wildner H, Müller T, Cho SH, Bröhl D, Cepko CL, Guillemot F, Birchmeier C. dILA neurons in the dorsal spinal cord are the product of terminal and non-terminal asymmetric progenitor cell divisions, and require Mash1 for their development. Development. 2006; 133:2105–2113. [PubMed: 16690754]

Wildner H, Das Gupta R, Bröhl D, Heppenstall PA, Zeilhofer HU, Birchmeier C. Genome-wide expression analysis of Ptf1a- and Ascl1-deficient mice reveals new markers for distinct dorsal horn interneuron populations contributing to nociceptive reflex plasticity. J. Neurosci. 2013; 33:7299–7307. [PubMed: 23616538]

Windhorst U. On the role of recurrent inhibitory feedback in motor control. Prog. Neurobiol. 1996; 49:517–587. [PubMed: 8912393]

Wootz H, Fitzsimons-Kantamneni E, Larhammar M, Rotterman TM, En-jin A, Patra K, Andre E, Van Zundert B, Kullander K, Alvarez FJ. Alterations in the motor neuron-renshaw cell circuit in the Sod1(G93A) mouse model. J. Comp. Neurol. 2013; 521:1449–1469.

Yokoi F, Cheetham CC, Campbell SL, Sweatt JD, Li Y. Presynaptic release deficits in a DYT1 dystonia mouse model. PLoS ONE. 2013; 8:e72491. [PubMed: 23967309]

Highlights

- Developmental lineage analysis localizes GABApre neurons to intermediate spinal cord

- Microarray screen identifies genes expressed in the GABApre population

- Dystonia-related genes *Klhl14* and *Tor1a* are expressed in the GABApre population

- Dystonia-causing *Tor1a* mutation *Dyt1 E* alters GABApre-sensory connectivity
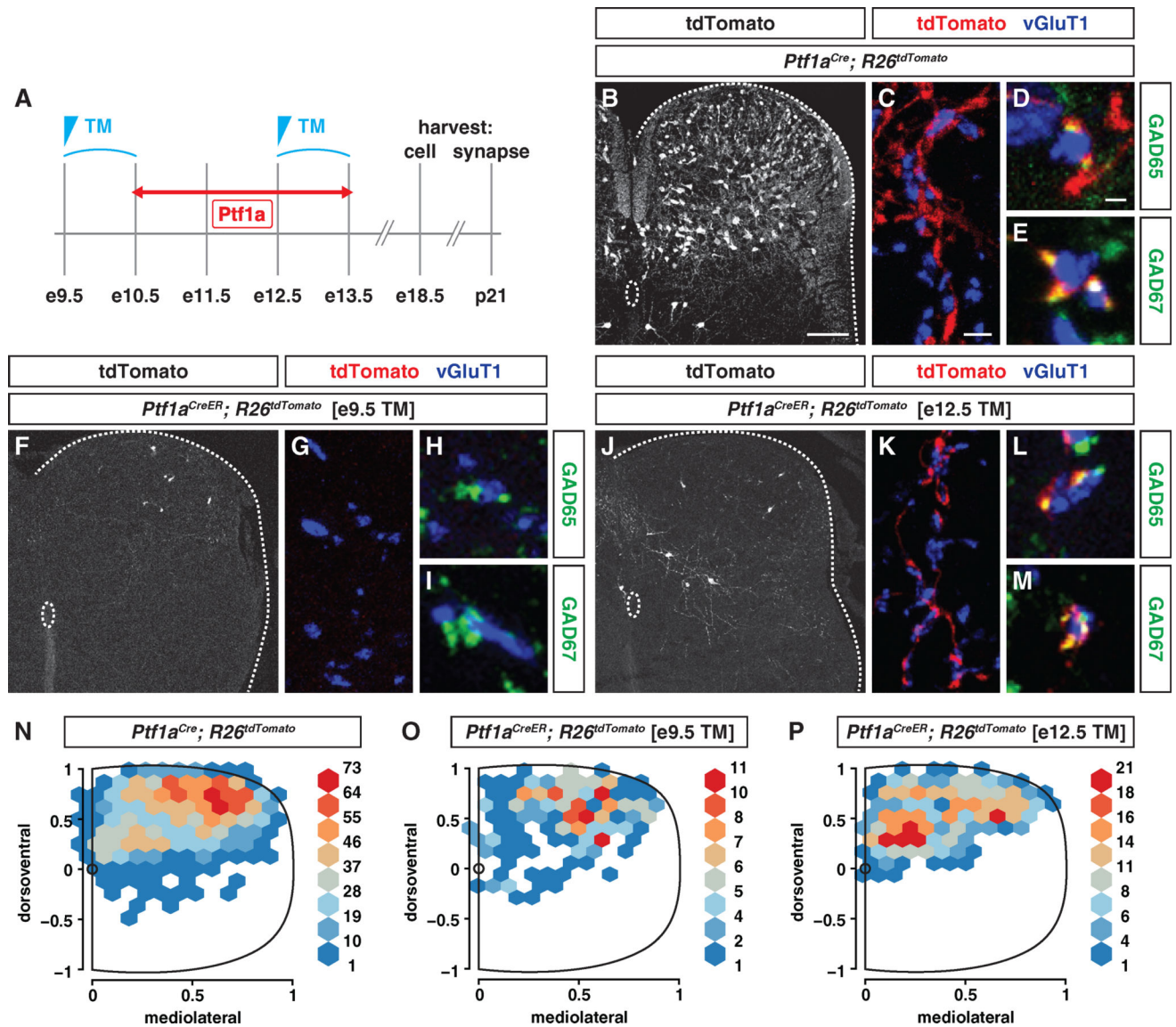
Figure 1. Late Ptf1a Expression Labels GABApre Neurons

(A) Ptf1a expression timeline and tamoxifen (TM) injection paradigm.

(B) tdTomato^{ON} cells in the dorsal-intermediate spinal cord of *Ptf1a^{Cre}; R26^{tdTomato}* mice at e18.5.

(C) tdTomato^{ON} (red) boutons on vGluT1^{ON} (blue) sensory afferent terminals in the ventral horn (lamina IX) of p21 *Ptf1a^{Cre}; R26^{tdTomato}* mice.

(D and E) tdTomato^{ON} (red) boutons on vGluT1^{ON} (blue) sensory afferent terminals in lamina IX of *Ptf1a^{Cre}; R26^{tdTomato}* mice co-express GABApre synaptic markers GAD65 (green, D) and GAD67 (green, E).

(F) tdTomato^{ON} cells in the dorsal spinal cord of e9.5 TM-injected *Ptf1a^{CreER}; R26^{tdTomato}* mice at e18.5.

(G–I) No ventral tdTomato^{ON} projections in e9.5 TM-injected *Ptf1a^{Cre}; R26^{tdTomato}* mice at p21 (G). No tdTomato co-expression with GABApre bouton markers GAD65 (green, H) and GAD67 (green, I).

(J) tdTomato^{ON} cells in the intermediate spinal cord of e12.5 TM-injected *Ptf1a^{CreER}; R26^{tdTomato}* mice at e18.5.

(K–M) tdTomato^{ON} (red) boutons project into the ventral spinal cord (K) in e12.5 TM-injected *Ptf1a^{Cre}; R26^{tdTomato}* mice at p21 and express GABApre synaptic markers GAD65 (green, L) and GAD67 (green, M).

(N–P) Distribution plots of tdTomato^{ON} neurons in three *Ptf1a^{Cre}; R26^{tdTomato}* (N), six e9.5 TM-injected *Ptf1a^{CreER}; R26^{tdTomato}* (O), and three e12.5 TM-injected *Ptf1a^{CreER}; R26^{tdTomato}* mice (P) at e18.5. Numbers represent absolute tdTomato^{ON} neuronal counts. Scale bars in (B), (F), and (J) represent 100 μm; scale bars in (C), (G), and (K) represent 3 μm; scale bars in (D), (E), (H), (I), (L), and (M) represent 1 mm.
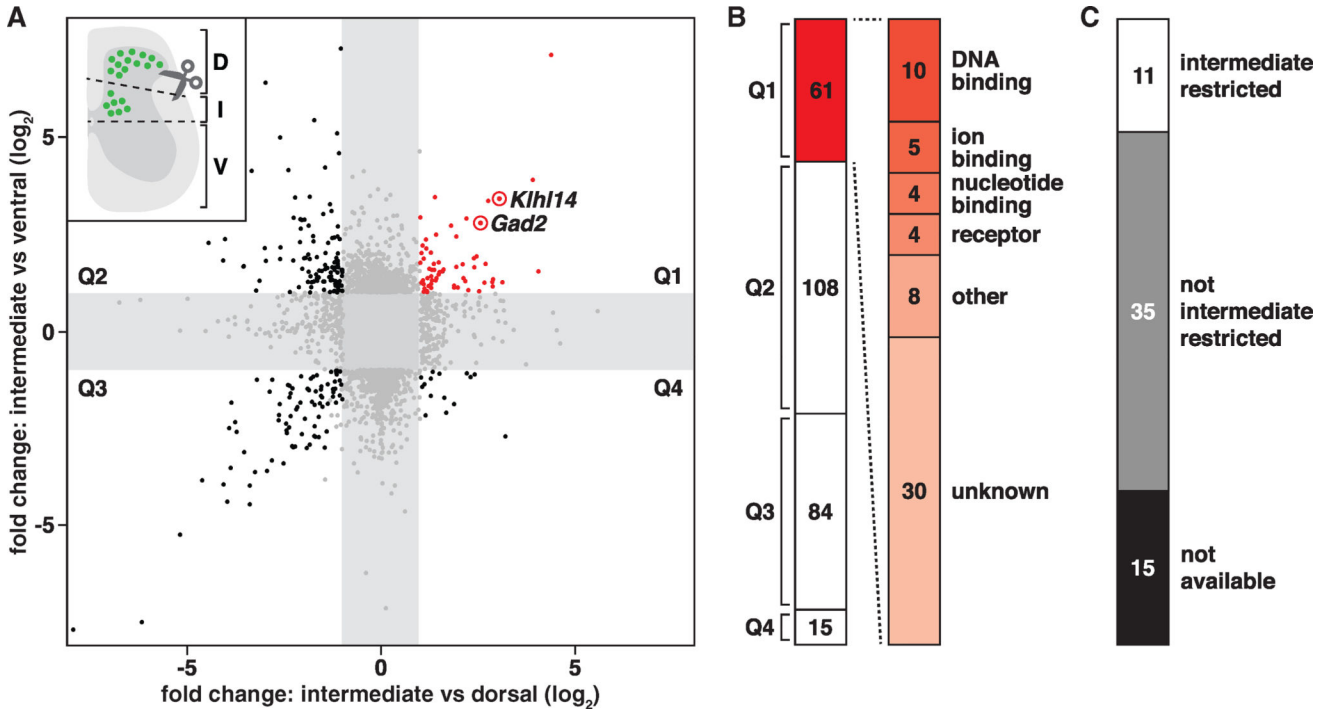
Figure 2. Screen for Novel Genes Expressed in the Intermediate Spinal Cord

(A) To find genes enriched in the intermediate spinal cord, gene expression levels were compared between dissected dorsal (D), intermediate (I), and ventral (V) spinal cord regions at p6 (see inset). Genes with significant ($p < 0.05$) and 2-fold or greater expression changes (268 genes) are graphed as a scatterplot comparing intermediate versus ventral (y axis) and intermediate versus dorsal (x axis) spinal regions. Genes that are upregulated in the intermediate region in both comparisons are in quadrant 1 (Q1, red, 61 genes); genes that are differentially expressed in both comparisons are in quadrants 2, 3, and 4 (Q2, Q3, and Q4, black, 207 genes); and genes that are differentially expressed in either comparison are gray (1,720 genes). Both *Gad2* and *Klhl14* are upregulated in the intermediate region (Q1).

(B) Functional classification of the 61 genes upregulated in both comparisons identified four main functional families and many other genes of unknown function or classification.

(C) Analyzing in situ hybridization data from the Allen Institute for Brain Science further restricted the 61 candidates to 11 genes (including *Klhl14*) that showed specific expression in the intermediate spinal cord.
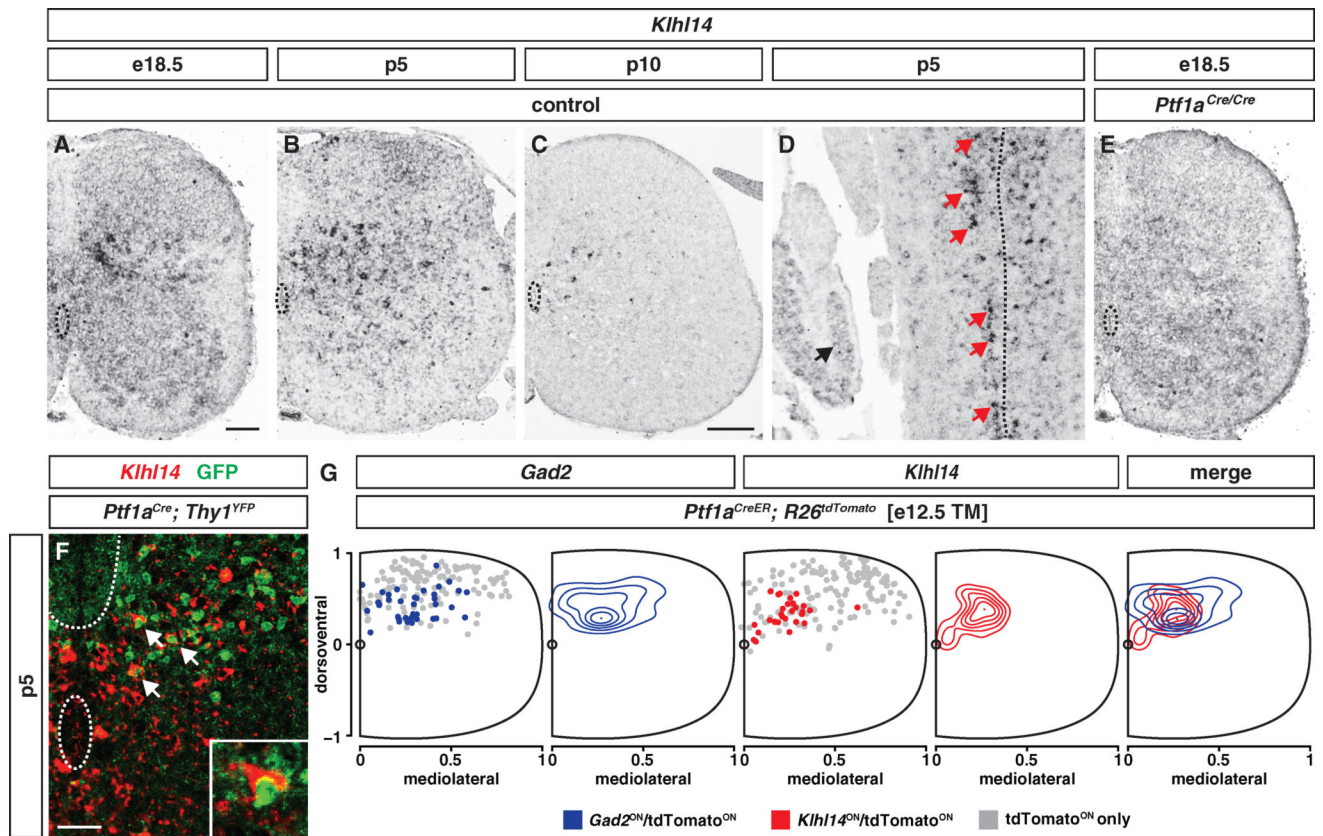
Figure 3. *Klhl14* Expression in Spinal Inhibitory Interneurons

(A–E) *Klhl14* transcript expression at e18.5 (A), p5 (B and D, red arrows), and p10 (C). There is no *Klhl14* expression in DRG (D, black arrow). Dotted line in (D) depicts midline. *Klhl14* expression is absent in e18.5 *Ptf1a* mutant (*Ptf1a*$^{Cre/Cre}$) spinal cords (E).

(F) *Klhl14* transcript co-expression with fluorescently labeled GFP^{ON} (green) neurons in the intermediate spinal cord of *Ptf1a*^{Cre}; *Thy1*^{YFP} mice at p5.

(G) Density plots of combined in situ and immunolabeling showing that at e18.5, *Gad2* (blue) expressing Ptf1a-derived cells in e12.5 TM-injected *Ptf1a*^{CreER}; *R26*^{tdTomato} mice settle in the intermediate spinal cord (n = 159 cells, three mice). *Klhl14* (red) expressing Ptf1a-derived cells in e12.5 TM-injected *Ptf1a*^{CreER}; *R26*^{tdTomato} mice settle in the intermediate spinal cord (n = 183 cells, three mice; see also Figures S2A–S2C). Ten to 20 sections per animal were analyzed and plotted in the same graph. *Gad2* (blue) and *Klhl14* (red) expression patterns in late Ptf1a-derived cells overlap.

Scale bars in (A), (B), and (E) represent 100 μm; scale bars in (C) and (D) represent 100 μm; scale bar in (F) represents 50 μm.
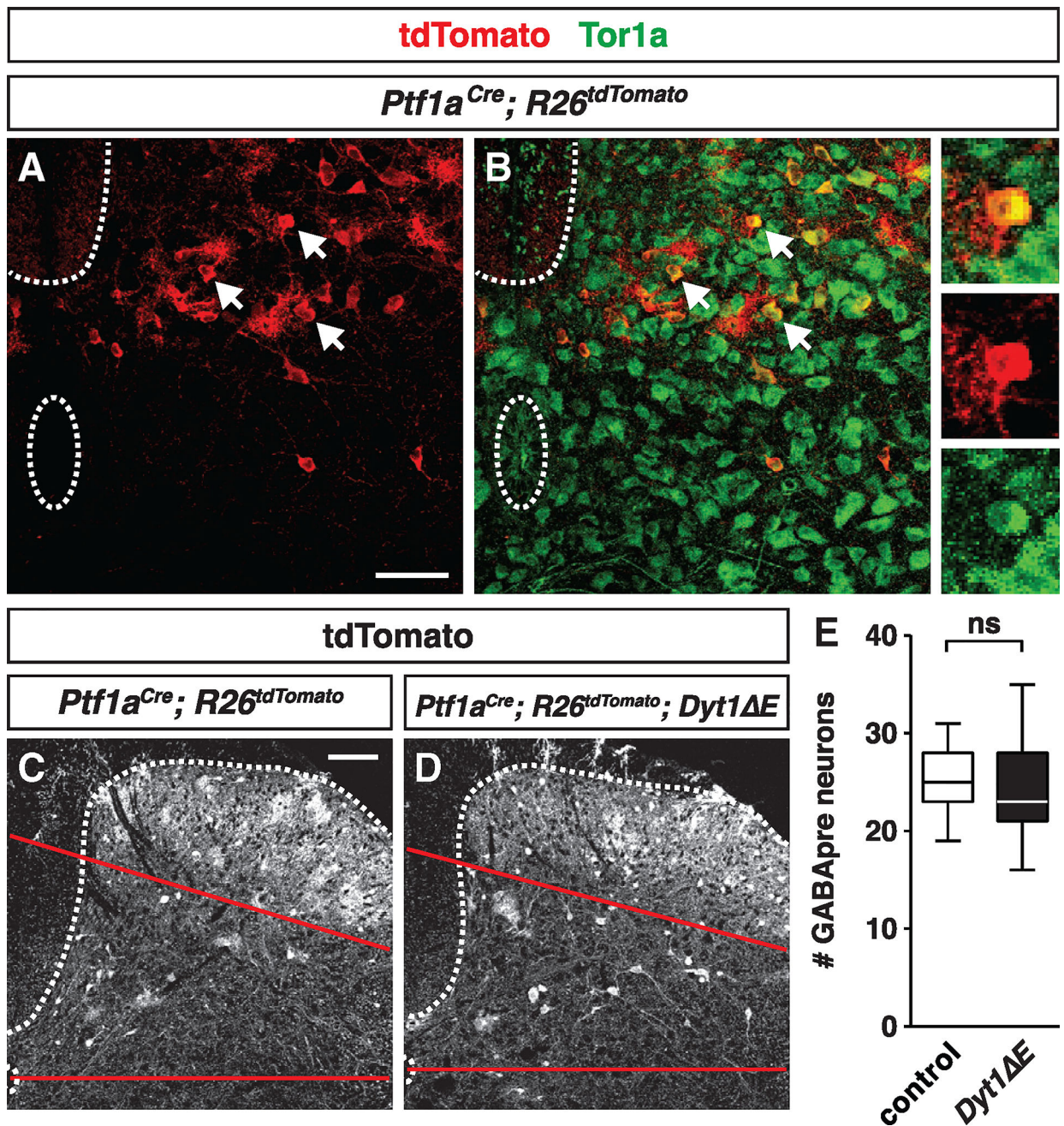
Figure 4. Normal GABApre Neuron Number in *Dyt1 E* Mice

(A and B) tdTomato^ON (red) neurons in the intermediate spinal cord of *Ptf1a^Cre; R26^tdTomato* mice. Tor1a (green, B) expression in tdTomato^ON (red, A and B) neurons in *Ptf1a^Cre; R26^tdTomato* mice at p5.

(C and D) tdTomato^ON cells in *Ptf1a^Cre; R26^tdTomato* control (C) and *Ptf1a^Cre; R26^tdTomato; Dyt1 E* (D) mice at p21. Red lines indicate approximate location of GABApre neurons.

(E) The number of putative GABApre neurons is normal in *Dyt1 E* mice compared with controls.

Scale bars in (A) and (B) represent 100 μm; scale bars in (C) and (D) represent 200 μm. Data are reported as mean ± SD.
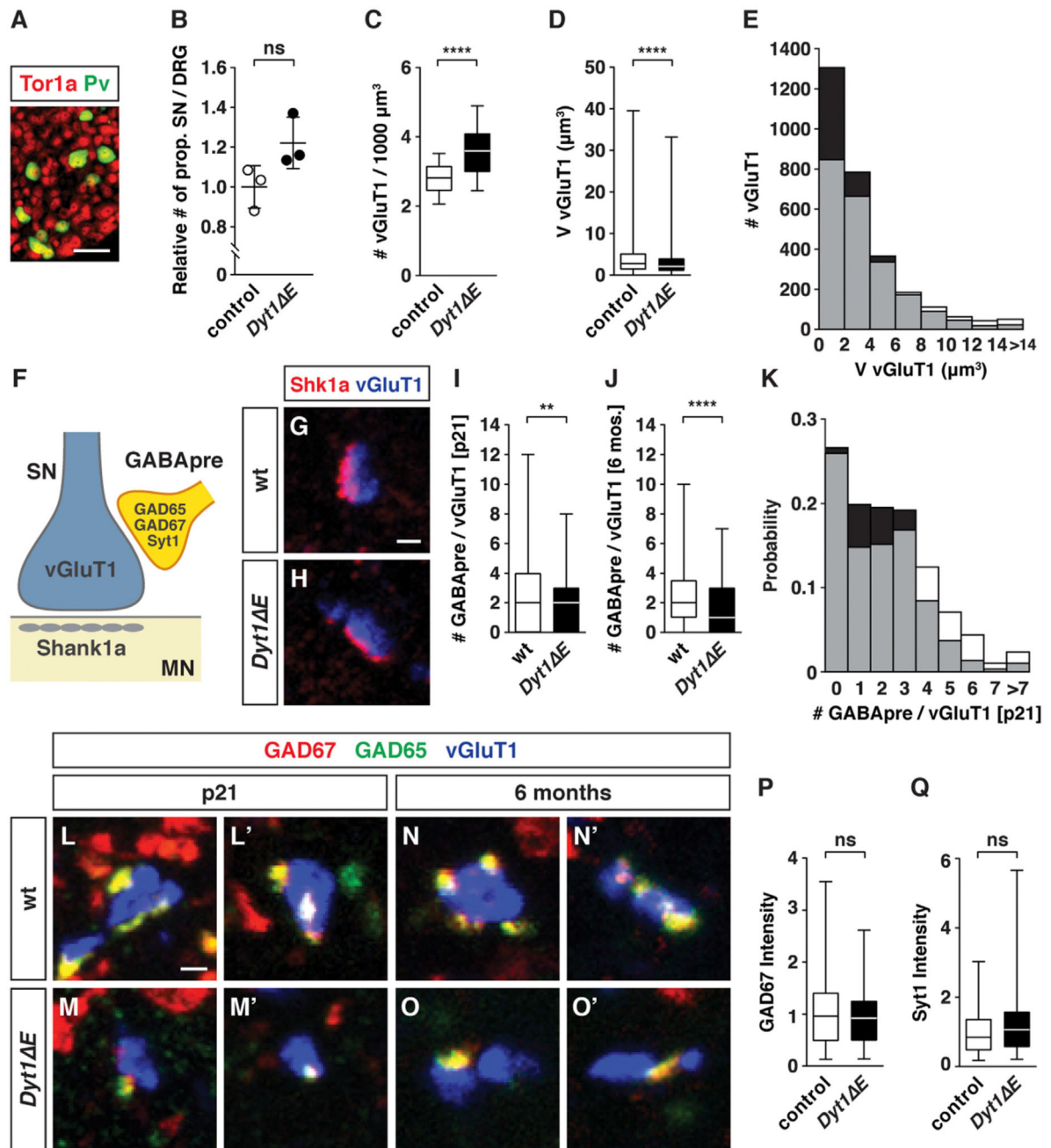
Figure 5. Abnormal GABApre Circuit Organization in *Dyt1 E* Mice

(A) Tor1a (red) is expressed in parvalbumin (Pv)-positive (green) proprioceptive sensory neurons in p6 DRG.

(B) The relative number of proprioceptive sensory neurons per DRG is unchanged between control (white) and *Dyt1 E* mice (black).

(C and D) Increased sensory afferent terminal density (C) and decreased volume (D) are seen in *Dyt1 E* mice compared with controls at p21.

(E) Histogram showing increased numbers of smaller volume sensory afferent terminals in *Dyt1 E* at p21 (control, white; *Dyt1 E*, black; overlap, gray).

(F) Schematic showing sensory neuron (SN) terminals express vGluT1 and are adjacent to Shank1a on motor neurons (MNs). GABApre boutons express GAD65, GAD67, and Syt1.

(G and H) vGluT1^{ON} (blue) sensory afferent terminals are adjacent to Shank1a (red) in WT (G) and *Dyt1 E* mice (H) at p21.

(I and L–M') Fewer GAD65^{ON} (green)/GAD67^{ON} (red) GABApre boutons (yellow) on vGluT1^{ON} (blue) sensory afferent terminals in p21 *Dyt1 E* mice (M and M') compared with WT mice (L and L'). Compiled average number of GAD65^{ON}/GAD67^{ON} GABApre boutons on vGluT1^{ON} sensory afferent terminals is reduced by 20.3% in *Dyt1 E* mice (I).

(J and N–O') Fewer GAD65^{ON} (green)/GAD67^{ON} (red) GABApre boutons (yellow) on vGluT1^{ON} (blue) sensory afferent terminals in 6-month-old *Dyt1 E* animals (O and O') compared with WT mice (N and N'). Compiled average number of GAD65^{ON}/GAD67^{ON} GABApre boutons on vGluT1^{ON} sensory afferent terminals is reduced by 27.4% in *Dyt1 E* mice (J).

(K) Histogram showing a shift in the ratio of GABApre boutons per vGluT1 terminal toward fewer GABApre/vGluT1 in *Dyt1 E* mice at p21 (control, white; *Dyt1 E*, black; overlap, gray).

(P and Q) Fluorescence intensity of GAD67 (P) and Syt1 (Q) is unchanged in *Dyt1 E* mice at p21.

Scale bar in (A) represents 50 μm; scale bars in (G) and (H) represent 1 μm; scale bars in (L)–(M') represent 1 μm. Data are reported as mean ± SD.